



## Durham E-Theses

---

# *EXPRESSION OF ENDOPLASMIC RETICULUM OXIDOREDUCTASES (EROS) AND THEIR ROLE IN THE GI TRACT*

WATSON, GRAEME

### How to cite:

---

WATSON, GRAEME (2012) *EXPRESSION OF ENDOPLASMIC RETICULUM OXIDOREDUCTASES (EROS) AND THEIR ROLE IN THE GI TRACT*, Durham theses, Durham University. Available at Durham E-Theses Online: <http://etheses.dur.ac.uk/5945/>

### Use policy

---

The full-text may be used and/or reproduced, and given to third parties in any format or medium, without prior permission or charge, for personal research or study, educational, or not-for-profit purposes provided that:

- a full bibliographic reference is made to the original source
- a [link](#) is made to the metadata record in Durham E-Theses
- the full-text is not changed in any way

The full-text must not be sold in any format or medium without the formal permission of the copyright holders.

Please consult the [full Durham E-Theses policy](#) for further details.

## **CHAPTER 3**

# **CHARACTERISATION OF THE OESOPHAGEAL CELLS OE21 AND OE33, AND THEIR EXPRESSION OF ER OXIDOREDUCTASES**

### 3.1 Introduction

The complex perturbed physiological environment in gastrointestinal tumours may involve redox proteins and metabolites, since oxidative damage has been implicated in GORD (Oh *et al.*, 2001). Suspected pathological mechanisms such as low pH and bile acids have been implicated in the generation of reactive oxygen species in Barrett's cells (Dvorak *et al.*, 2007, Si *et al.*, 2007). The consumption of glutathione may be involved in the increase in expression of oxidative stress genes, as glutathione can be used to conjugate and inactivate carcinogens (Stoner *et al.*, 2008).

The mechanisms of how transformed oesophageal cells are able to persist and proliferate in this harsh environment are unclear, and are of interest to the field of oxidative protein folding. In hypoxic tumours, such as adenocarcinoma of the upper GI tract, it was observed that Ero1 $\alpha$  is upregulated in tumour cell lines and mouse embryonic fibroblasts following hypoxia and hypoglycaemia in normoxia, which are known consequences of adenocarcinoma (Griffiths *et al.*, 2007, May *et al.*, 2005b). Ero1 $\alpha$  upregulation was shown to be mediated by the hypoxia-inducible factor 1 (HIF1) transcription factor. In addition, the secretion of the disulphide-bond containing vascular endothelial growth factor, (VEGF) was impaired in hypoxia, and partially restored by supplementation with diamide, an oxidising equivalent (May *et al.*, 2005b). In tumour sections (mouse teratomas and human breast carcinomas) Ero1 $\alpha$  was co-expressed with VEGF, visualised by *in situ* hybridisation. The study concluded that in hypoxic tumours, increased Ero1 $\alpha$  expression may serve to improve VEGF secretion, and suggests Ero1 $\alpha$  as a potential anti-angiogenic target (May *et al.*, 2005a). As such, Ero1 $\alpha$  represents not only a candidate marker for Barrett's adenocarcinoma but also the GI system presents an environment in which the role of Eros can be studied further.

## 3.2 Results

### 3.2.1 Characteristics and appearance of the cell lines HT1080, OE21 and OE33

The initial exploration of ER oxidoreductase expression patterns in upper GI tissues utilised the GI cells lines OE21 and OE33 (European Collection of Cell Cultures, Porton Down, Salisbury, Wiltshire, U.K.). OE21 is derived from squamous carcinoma of mid oesophagus from a 74 year-old male patient. The tumor was assigned pathological stage IIA (UICC) and had moderate differentiation. OE33 was derived from adenocarcinoma of the lower oesophagus following Barrett's metaplasia from a 73-year-old female patient. The tumor was also pathological stage IIA (UICC) and had poor differentiation. (Rockett *et al.*, 1997). As such OE21 and OE33 serve as a model for comparison between GI tumours that are either non-secretory or secretory, and are a good target to compare oxidoreductase expression. The HT1080 cell line (ECAC) was cultured as a non-GI control, and was obtained from a fibrosarcoma (Rasheed *et al.*, 1974).

While HT1080 cells are well-characterised in the lab, OE21 and OE33 lines were being used for the first time, so initial experiments focussed on their characteristic features, including growth rates and cell morphology. Both these cell types have been used in the field of upper GI cancer, either to serve as a model cell line or in identification of candidate biomarkers (Jenkins *et al.*, 2004, Mariette *et al.*, 2004, Edmiston *et al.*, 2005, Wong *et al.*, 2005, Duggan *et al.*, 2006, Hao *et al.*, 2006, Onwuegbusi *et al.*, 2007, Liu *et al.*, 2007, Jenkins *et al.*, 2008, Peng *et al.*, 2009).

The HT1080 fibrosarcoma cells were passaged ~80% confluence, at a 1:9 split (10 ml culture), every 3-4 days, and are shown in Figure 3.1A. The OE21 and OE33 cells were



passed every 3-4 days at 80% confluence, at a 3:7 split (10 ml culture). Growth was poor if the oesophageal cells were passed at a lower ratio, including a 2:4 split. The OE21 cells could form a confluent monolayer (Figure 3.1B), whereas the OE33 cells grew as a patchwork which seldom reach confluence across the dish (Figure 3.1C).

### **3.2.2 Basal expression of oxidoreductases and PDIs in oesophageal cell lines**

Having established the cell lines in culture, the expression of Ero1 $\alpha$  in these lines was examined. Endogenous Ero1 $\alpha$  had previously been detected in the HT1080 cell line, and also showed differential expression in human oesophageal and stomach tissue sections obtained from both a commercial source (Medical Solutions, Nottingham, UK), and from the pathology department of James Cook University Hospital (JCUH) (Dias-Gunasekara and Benham, unpublished, 2006-2007).

In transfected cells, Ero1 $\alpha$  exists in at least three states, including two oxidised forms, OX1, OX2 and a reduced form (Benham *et al.*, 2000). In general, proteins in the non-reduced form have disulphide bonds that remain intact when trapped by an alkylating agent, and run lower on an SDS-PAGE gel. In the reduced form, proteins run slightly higher when its disulphide bonds are broken by DTT. This is illustrated schematically in Figure 3.2. When OE33 lysates were analysed by Western blotting for Ero1 $\alpha$  under non-reducing conditions (Figure 3.3, lane 1) or reducing conditions (Figure 3.3, lane 4) a clear difference could be seen in the migration of Ero1 $\alpha$ , indicating the presence of structural disulfide bonds. By loading a small amount of DTT adjacent to a non-reduced sample of an Ero1 $\alpha$  containing lysate, the DTT partially reduces the non-reduced sample, having diffused across the lane (Figure 3.3, lane 2). Note that Ero1 $\alpha$  in OE33 cells was almost exclusively in the most compact OX2 state (Figure 3.3, lane 1).

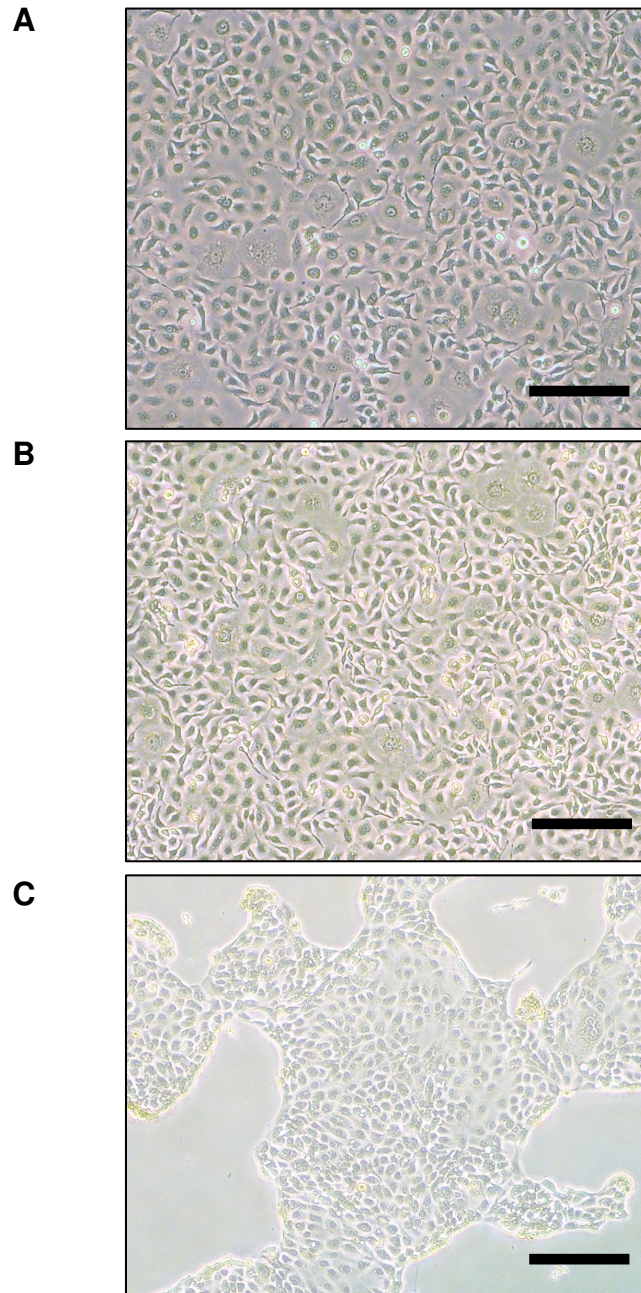


Figure 3.1 Appearance of the cell lines HT1080, OE21 and OE33 (phase contrast microscopy)

A: HT1080, derived from human fibrosarcoma; B: OE21, derived from human oesophageal squamous carcinoma; C: OE33, derived from human oesophageal adenocarcinoma, grew in large clumps. Scale bar: 500  $\mu\text{m}$ .

For a comparison of oxidoreductase, chaperone and client protein expression, cell lysates from HT1080, OE21 and OE33 were probed for Ero1 $\alpha$ , PDI, ERp57, ERp72, HSP90 and MHC class I (Figure 3.4A-F). Relative to HT1080, the non-GI control cell line, Ero1 $\alpha$  expression was stronger in OE33, and weaker in OE21 (Figure 3.4A). In contrast, PDI and ERp57 expression were similar across all cell lines (Figure 3.4B-C). The band that ran above PDI in the reducing gel was from known antibody cross reactivity with FCS, and was seen in the non-reducing gel underneath PDI. In addition, no changes in oxidation state were expected in ERp57 as it contains no structural disulphide bonds.

The blot of ERp72 suggested a slightly lower expression in OE21 relative to either HT1080 or OE33, correlating with the expression pattern of Ero1 $\alpha$  (Figure 3.4D). High expression of HSP90 has been seen in oesophageal adenocarcinoma and represents a potential therapeutic target in other studies (Wu *et al.*, 2009), though expression between HT1080, OE21 and OE33 here was similar (Figure 3.4E). Finally, the classical disulphide bonded MHC class I proteins were expressed much higher in the OE33 cells than either HT1080 or OE21 (Figure 3.4F).

The initial data from Western blotting showed that there was a differential expression of Ero1 $\alpha$  and possibly ERp72 between OE21 and OE33 cells at steady state, although this was not the case for PDI, or another one of its family members, ERp57.

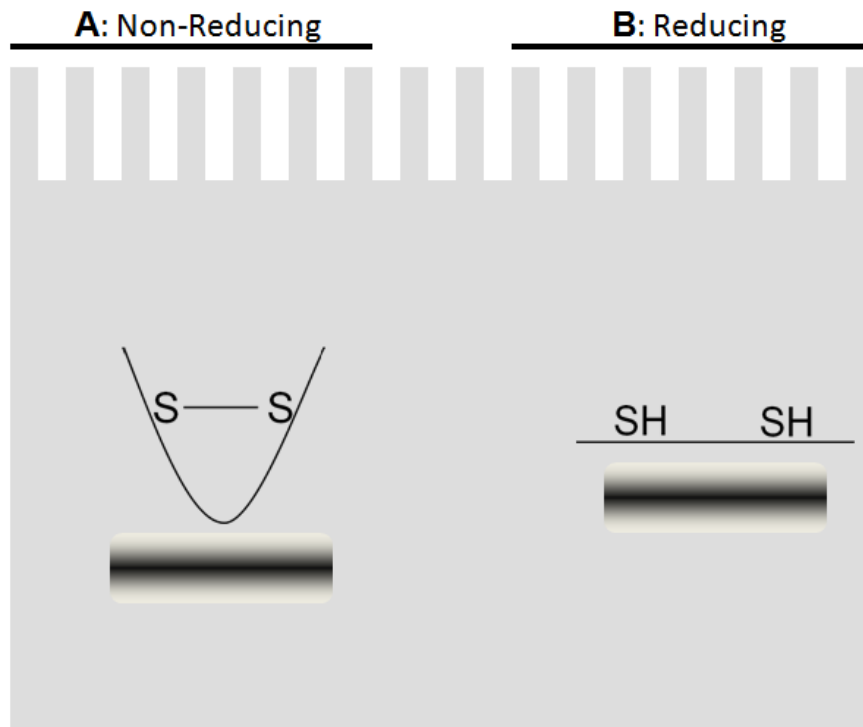


Figure 3.2 Schematic of non-reduced and reduced proteins in SDS-PAGE

A: In non-reducing SDS-PAGE, the protein's disulphide bonds are intact, and run lower on the gel as they are more compact. If different oxidation states are present, these will also be visualised on gel. B: In reducing SDS-PAGE, disulphide bonds are broken by DTT and trapped by an alkylating agent. The proteins are more linear as a result, run higher on the gel, and multiple oxidation states can be resolved to a single band.

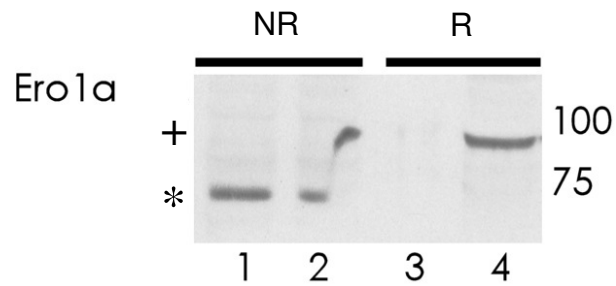
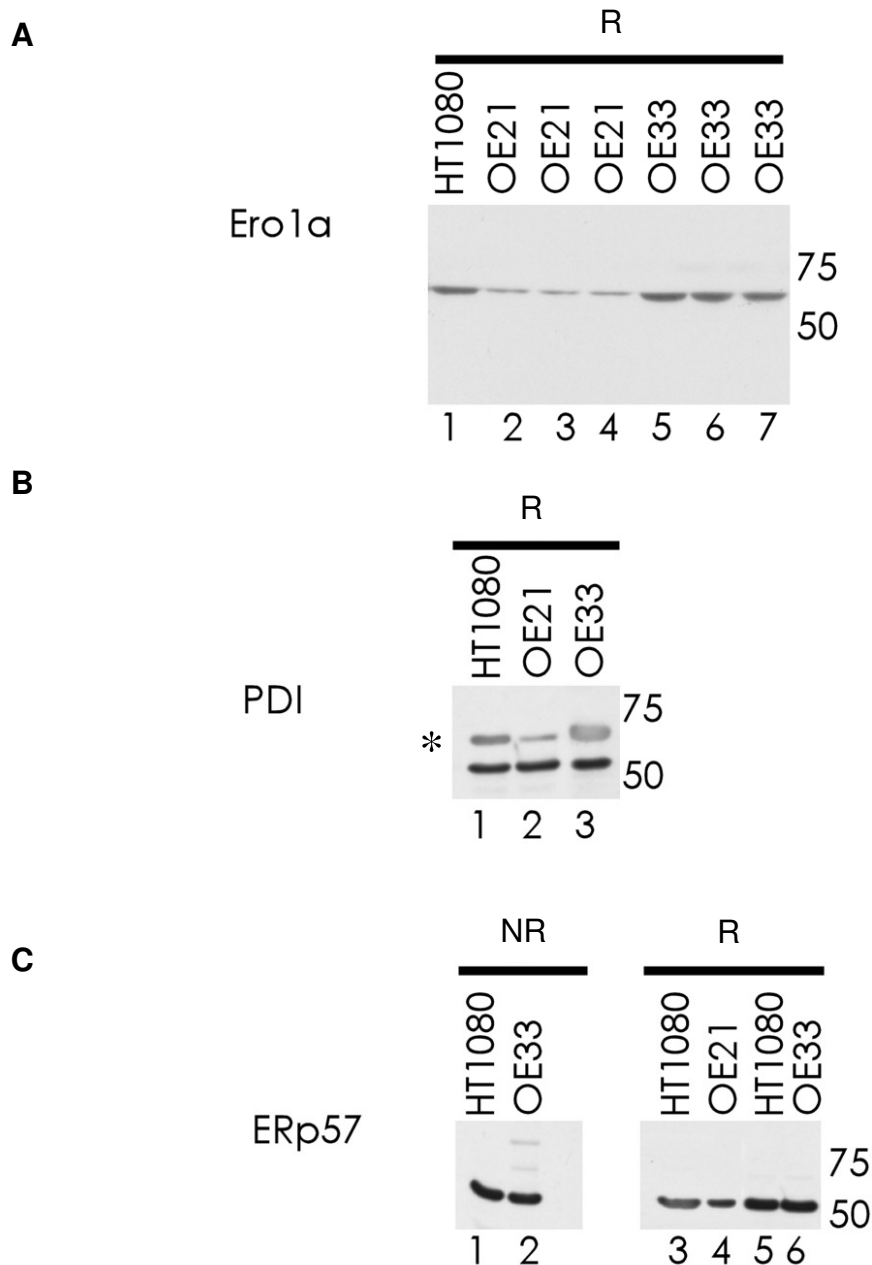


Figure 3.3 Ero1 $\alpha$  can be reduced *in vitro* with the reducing agent dithiothreitol

Western blot for Ero1 $\alpha$ , with all samples from untreated OE33 cell lysate. In the non-reduced portion of the gel (lanes 1 and left part of lane 2), Ero1 $\alpha$  exists in the Ox2 state (Benham *et al.*, 2000). In the non-reduced cell lysate, the disulphide bonds of Ero1 $\alpha$  are trapped by the alkylating agent, NEM. Ero1 $\alpha$  can be reduced in the presence of DTT, loaded in the lane marked \*. DTT breaks disulphide bonds present within Ero1 $\alpha$ , which are trapped by the NEM alkylating agent present in the original lysis buffer. As a consequence, Ero1 $\alpha$  runs higher on the gel (lane 4), and the left portion of lane 2 is raised upwards.



**Figure 3.4** Expression profiles of Ero1 $\alpha$  and PDI in HT1080, OE21 and OE33

A: Anti-Ero1 $\alpha$  serum (monoclonal antibody 2G4) detected the reduced form of Ero1 $\alpha$ , consistently expressed higher in untreated OE33 cells. B: The polyclonal anti-PDI serum showed the reduced form of PDI. The grey bands around 70 kDa were background bands \*. C: ERp57 expression between untreated HT080, OE21 and OE33. No additional oxidation states of ERp57 were seen in the non-reducing gel, as expected.

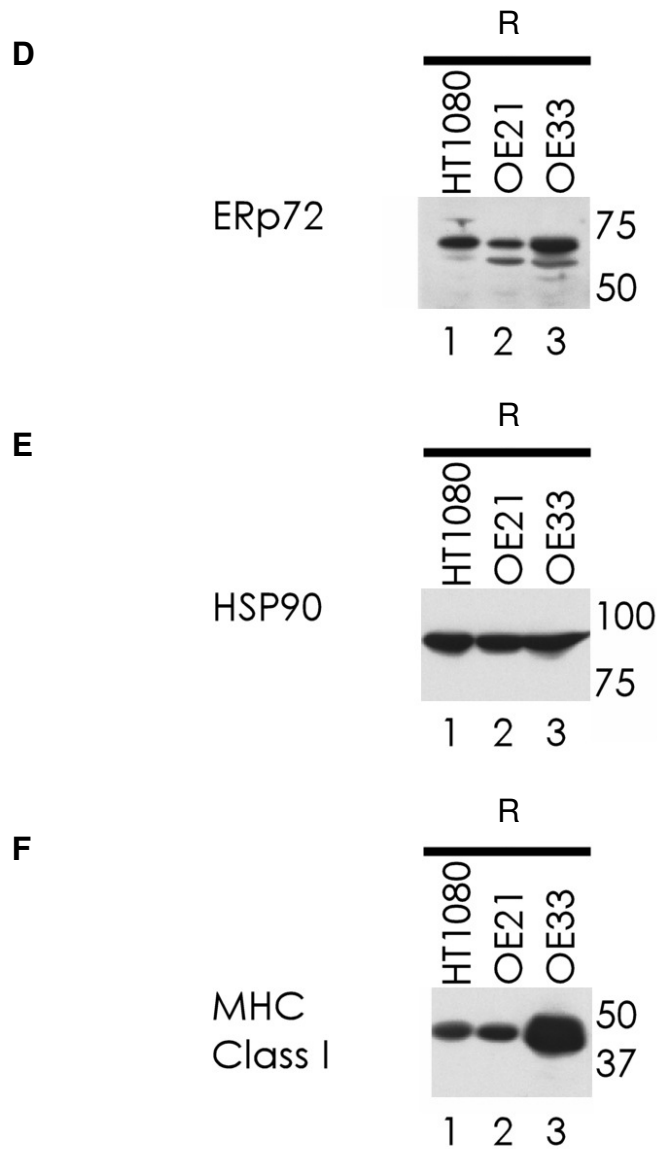


Figure 3.4 (cont) Expression profiles of Ero1 $\alpha$ , PDI, ERp57, ERp72, HSP90 and MHC class I in HT1080, OE21 and OE33

D: Western blot for ERp72; note the background band that runs beneath detectable ERp72. E: Western blot for HSP90; expression is similar between non- and GI-cell types. F: MHC class I expression is similar between HT1080 and OE21, though expression in OE33 is much higher.

### 3.2.3 Transfection of HT1080, OE21 and OE33 cell lines with Ero1 $\alpha$ -myc

In order to explore the significance of, and difference in Ero1 $\alpha$  expression between OE21 and OE33, a series of transfection experiments were carried out to determine the transfectability of the cells, and hence their amenability for overexpression and knockdown experiments.

Initially, Ero1 $\alpha$ -myc cDNA was purified from bacterial plasmids using the Qiagen Mini/Maxi-Prep procedure. HT1080 cells were transfected using lipofectamine 2000. Post nuclear cell lysates were analysed by SDS-PAGE and Western blotting, confirming that HT1080 cells were successfully transfected (compare lanes 1 and 2, Figure 3.5A). Lane 1 shows endogenous Ero1 $\alpha$ , while lane 2 shows both endogenous Ero1 $\alpha$  as lane 1, and an upper band corresponding to the expression of the myc-tagged Ero1 $\alpha$  construct. The upper band present in lane 2 was the myc-tagged Ero1 $\alpha$ . Tagged Ero1 $\alpha$  could also be seen when the membrane was probed with a monoclonal myc antibody (Figure 3.5B). In this figure, the untransfected sample (lane 2) showed no expression of myc, as expected. Myc expression was seen both in the positive control (lane 1) and the transfected cells (lane 3).

Another transfection reagent, genejuice, was also used to test its effectiveness in transfection compared to lipofectamine 2000 (Figure 3.5C). The manufacturers typically recommend the use of 15  $\mu$ l genejuice with 5  $\mu$ g of DNA in 4 ml, so a titration series was set up to verify this, and to see if a lower amount of genejuice would be sufficient. Negative controls for transfection (lanes 1 and 2, Figure 3.5C) showed no signal as expected. An Ero1 $\alpha$ -myc positive sample from a lipofectamine transfection (lane 3) was compared to Ero1 $\alpha$ -myc transfected with 10, 15, and 20  $\mu$ l of genejuice (lanes 4, 5 and 6). It was clear that 10  $\mu$ l of genejuice was insufficient for transfection, and that 15  $\mu$ l was sufficient to ensure a positive result, as the signal was not improved



further with 20  $\mu$ l of genejuice. When compared with lipofectamine, there appeared to be no increase in expression or differences in terms of cell death (not shown).

Having established the reagents in HT1080 cells, the OE21 and OE33 cell lines were subjected to transfection. Figure 3.5D shows a transfection titration of lipofectamine 2000, keeping DNA concentration constant. In all treatment groups, endogenous Ero1 $\alpha$  was expressed, (faint lower band on the reducing gel). In OE21, lipofectamine used at 1  $\mu$ l or 2.5  $\mu$ l was not sufficient to transfect Ero1 $\alpha$ -myc DNA. (Figure 3.5D, lanes 2 and 3). A number of titrations and optimisations were carried out in each of the cell lines, though the oesophageal cell lines proved weakly transfectable with Ero1 $\alpha$  according to the standard protocol.

Because the oesophageal lines were poorly transfectable using conventional protocols, a modified protocol was established after further optimisation experiments (these transfectants are shown in Chapter 4). In this protocol, cells were seeded at high density, and allowed to settle for 3 hours until they had adhered. As rounded cells, the OE cell lines could be transfected more readily, but it was not possible to reproducibly analyse the effects of overexpression of Ero1 $\alpha$  (in OE21 cells) or knockdown of Ero1 $\alpha$  (in OE33 cells) on the function and expression of oxidoreductases in these cell lines.

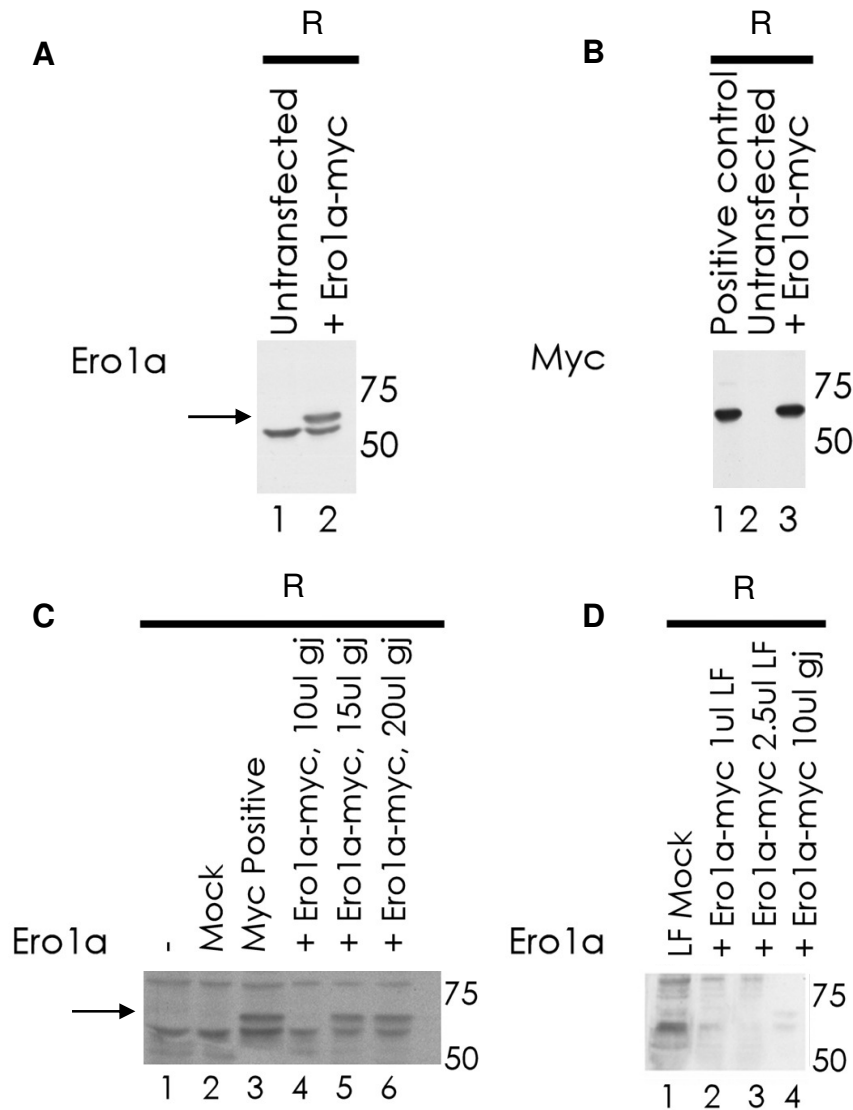


Figure 3.5 Western blots from transfection experiments

HT1080 cells transfected with Ero1 $\alpha$ -myc were analysed by SDS-PAGE/Western blotting. A: Western blot for Ero1 $\alpha$ : Note the second upper band in the right hand lane is Ero1 $\alpha$ -myc, distinct from its lower running, wildtype counterpart (see arrows in A and B). B: Western blot for myc; a known myc positive control is shown in lane 1 and lane 3, a verified Ero1 $\alpha$ -myc transfectant. C: HT1080 cells were left untransfected (lane 1), mock transfected (lane 2), or transfected with the given amounts of genejuice (gj; lanes 4-6). The expression of Ero1 $\alpha$  was determined by Western blotting with D5 compared with a known positive lysate (lane 3). D: A D5 probe showing a comparison between lipofectamine and genejuice transfection in OE21 cells.

### **3.3 Using cell culture models of reflux and gastrointestinal cancer to explore expression of oxidoreductases and protein disulphide isomerases**

A key feature of Barrett's oesophagus is the presence of stomach acid in the refluxate, which is associated with the change from a stratified squamous to columnar epithelium. In order to test if the pH of the medium exerted an effect on the expression, oxidation state, or interactions of various ER chaperones, a series of experiments were carried out to assess cell viability at low pH, and also to obtain protein expression data.

#### **3.3.1 Alteration of pH to determine the effect on cell viability and ER protein expression**

The HT1080 cell line was initially cultured in altered pH conditions, to optimise the techniques and as a non-GI control to which the OE21 and OE33 cells could be compared. To explore pH sensitivity in HT1080, OE21 and OE33, cells were treated with different pH media and post-treatment viability assessed. The cells cultured in low pH conditions had a similar morphology to the control cells, even comparing the pH 1 treated cells to control (Figure 3.6). In all cell lines, some cells remained adhered to the dish, although HT1080 seemed to have lost more cells during treatment than either of the OE cells, and had an elongated appearance when treated between pH 1-3 (Figure 3.6). Since strong acids and alkali conditions are likely to kill or fix cells, cell viability and morphology was explored using trypan blue and crystal violet staining, and also by re-seeding cells following pH treatment, and by seeding them directly into acid medium. In a follow-up experiment, ~70% confluent dishes of OE21 and OE33 cells were treated for 24 hours in pH 1, pH 2 or normal media in duplicate. One set were stained with Trypan blue *in situ*, and the second set were stained with crystal violet, and lysed in 1% SDS (Yamamoto *et al.*, 2007). When the pH 1 and 2 treated cells stained with

trypan blue *in situ* were visualised, it was clear that the entire monolayer consisted of dead cells, when compared to control (Figure 3.7). A 1 in 1000 dilution of crystal violet SDS lysate was examined by spectrophotometry at OD 600, to measure the release of crystal violet from the cells. The crystal violet assay did not discriminate between living and pH fixed cells, giving very similar OD 600 between samples (not shown). To further examine cell viability after pH treatment, OE21 and OE33 cells were grown to ~70% confluence, treated for 24 hours with pH 1-7 or normal medium, and then trypsinised following HBSS and DPBS washing steps. The total cell suspensions were then added directly to 4ml fresh medium in a new dish. OE21 and 33 cells treated with pH 1, 2 media were fixed and would not trypsinise. Cells treated with pH 3 media partially trypsinised, but were not adherent the following day along with pH 4 treated cells, which had trypsinised. Cells incubated with pH 5-pH 7 media were viable. After 24 hours, the cells were then examined and stained with trypan blue *in situ* (Figure 3.8). Rather than grow the cells to confluence and then treat, an alternate pH media treatment was carried out whereby the OE21 and OE33 cells were seeded directly to dishes containing pH 4-7 or normal media. After 24 hours, only the cells treated at pH 5-7 adhered to the dish. As both cell lines showed non-adherent, floating cells at pH 4, pH 5 was taken to be the threshold of tolerance for viability for OE21 and OE33. Trypan blue staining (Figure 3.8) showed that the majority of cells treated at pH 5-7 were, in fact, viable, despite a few dead (blue) cells. An estimate of percentage cell death based on field of view counts in treated OE21 and OE33 cells is shown in Figure 3.9. The proportion of dead cells was larger in pH 5 treated OE33 cells. In conclusion, the OE cells could not tolerate medium with a pH below 6.

Having established the pH sensitivity of the cell lines, Ero1 $\alpha$  and PDI expression was then determined within this range. HT1080 cells were grown to ~70% confluence in 6cm dishes, washed with DPBS, and were subjected to a 24 hour treatment in DMEM

which had been altered to pH 6.5, pH 7, pH 7.5 or pH 8.5. The control treatment was standard DMEM (pH 7.96). Following treatment, the old medium was tested with pH paper to see if pH had changed during the time-course, but no significant changes were seen. The cells appeared to have normal morphology. Figure 3.10 shows PDI expression analysed by Western blotting in these treated HT1080 cells. The reducing gel (lanes 1-5) shows that PDI expression was unchanged as a result of treatment. The non-reducing gel (lanes 6-10) shows a band present in each sample at around 100 kDa, which appeared more strongly in the treated cells. This band was notably less at pH 7, with a 150kDa band taking precedence. This experiment suggested that PDI might be subject to pH induced changes in its binding partners, and hence this was further investigated in the OE cell lines.

OE21 and OE33 cells at ~70% confluence in 6cm dishes were treated with pH 6.5, pH 7, pH 7.5 or pH 8.5 for 24 hours. The control treatment was standard RPMI 1640 (pH 8.25). Ero1 $\alpha$  and PDI expression in these treated cells is shown in Figure 3.11A and B, respectively. The expression of Ero1 $\alpha$  was not influenced by pH in either the OE21 (Figure 3.11A lanes 1-5) or OE33 cells (Figure 3.11A, lanes 6-10). OE33 showed a slightly weaker signal for Ero1 $\alpha$  after pH 8.5 treatment (Lane 10) but this is not believed to reflect an expression change following further experiments. Similarly, PDI did not show a change in expression as a result of altering pH conditions, relative to control, in either OE21 or OE33 cells (Figure 3.11B). Under non-reducing conditions, the Ero1 $\alpha$  signal from the OE21 samples was hardly visible. This was often the case in Ero1 $\alpha$  OE21 blots probed with the D5 polyclonal antibody (compare to monoclonal 2G4 Figure 3.3A), and may reflect epitope availability and/or complex formation, coupled with the generally low expression of Ero1 $\alpha$  in this cell line.

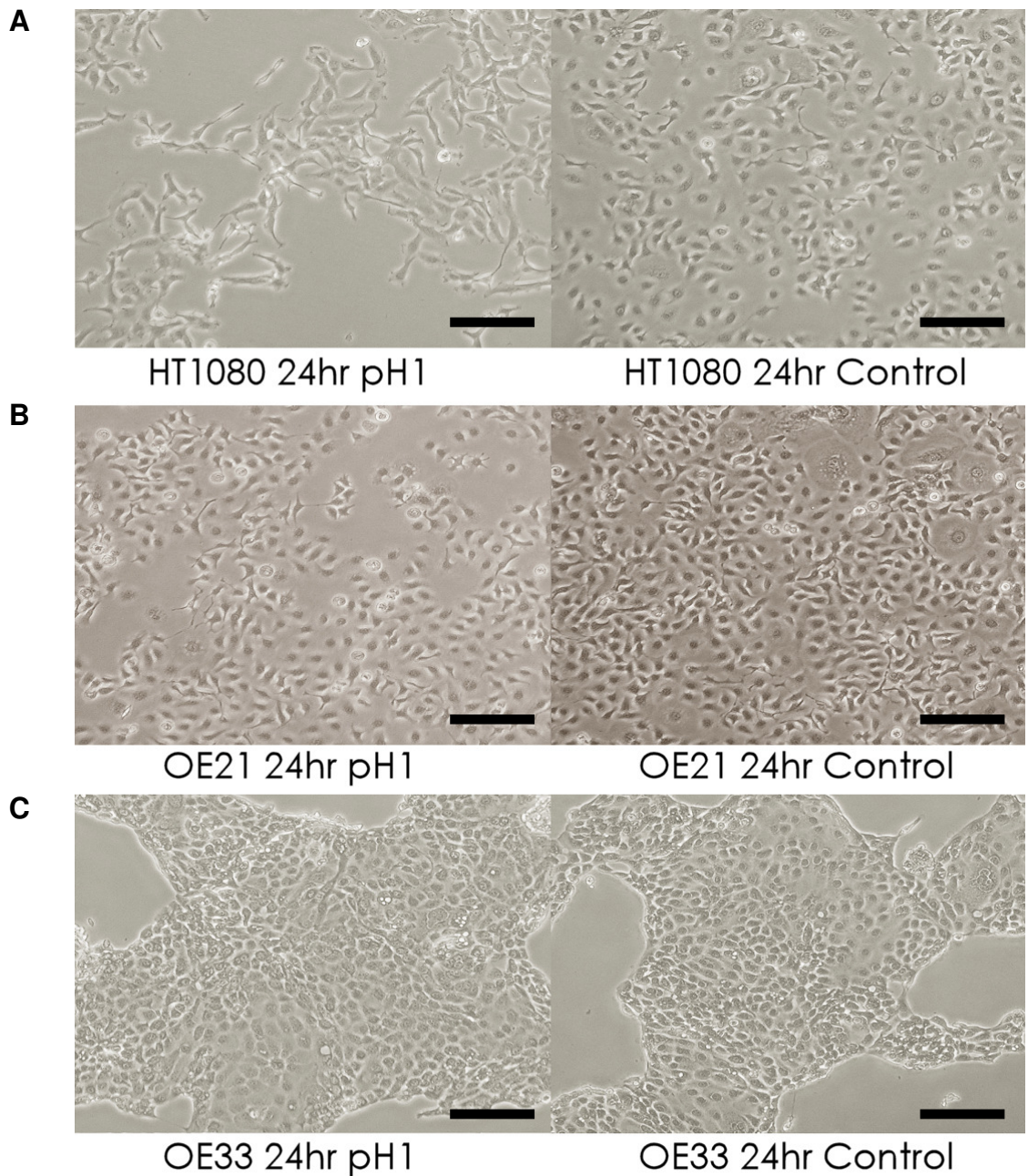


Figure 3.6 HT1080, OE21 and OE33 pH 1 24 hour treatment

A: HT1080 B: OE21 and C: OE33 cells at pH 1, compared to standard medium control, over 24 hours. Scale bars: 500  $\mu$ m.

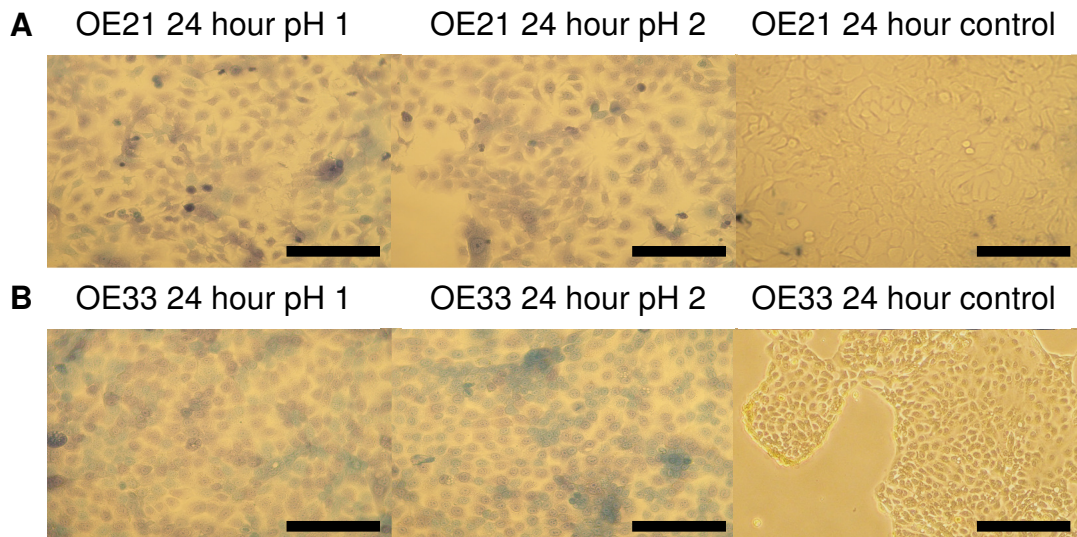


Figure 3.7 OE21 and OE33 pH 1 and 2 24 hour treatment compared to control

OE21 cells and OE33 cells grown to ~70% confluence, treated with acid media and stained with Trypan blue. In both A: OE21 and B: OE33 pH 1 and 2 treatment caused death, and the cells remained fixed to the dish. The large dark areas on OE33 are from trypan blue precipitate. Scale bars: 500  $\mu\text{m}$ .



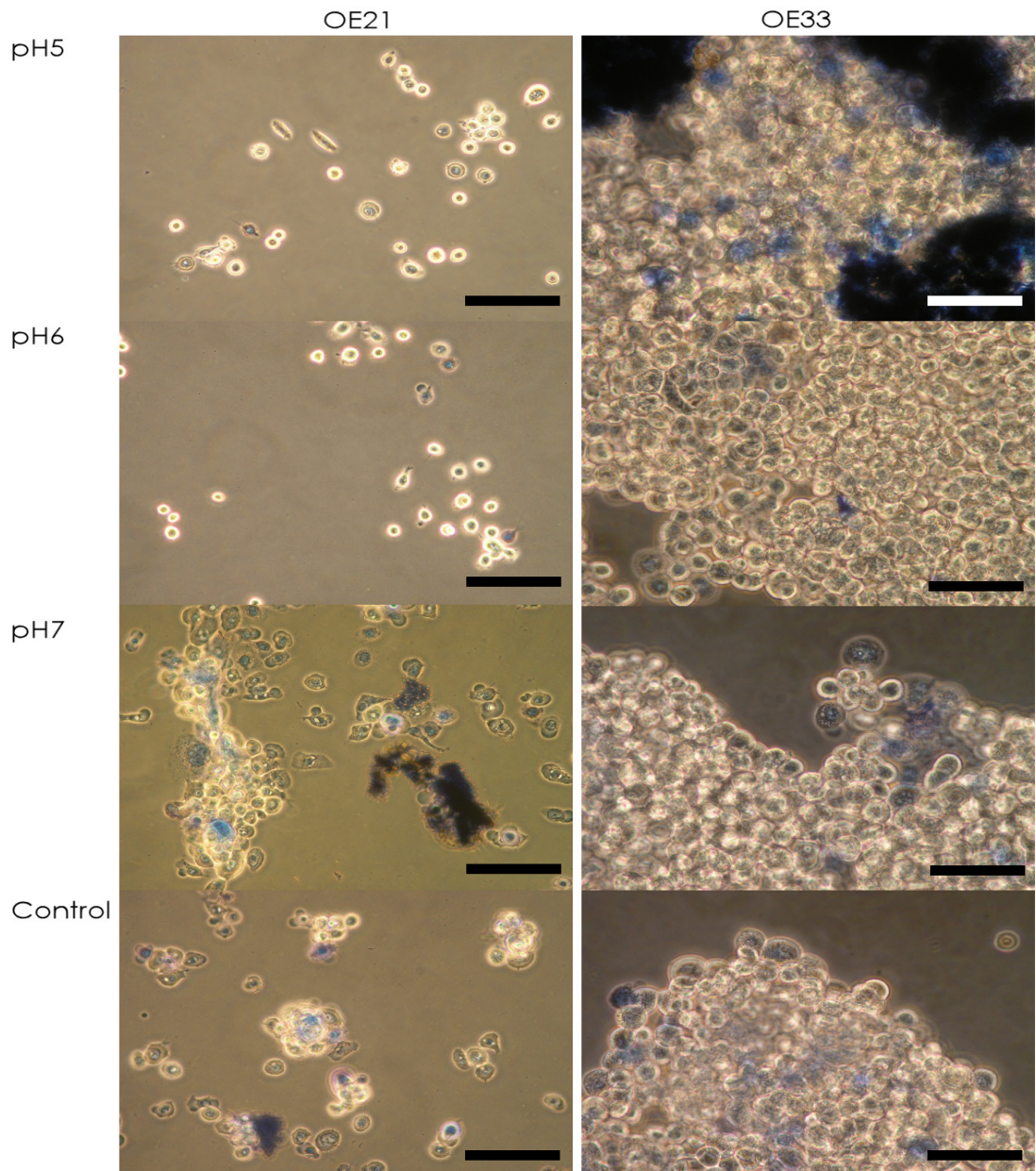


Figure 3.8 Trypan blue stained OE21 and OE33 pH 5-7 treated cells

Trypan blue stained cells following culture in pH 5, 6 and 7 media, and standard media. The blue staining indicates dead cells. Untreated controls are shown at the bottom of the figure. Scale bars: 100  $\mu\text{m}$ .



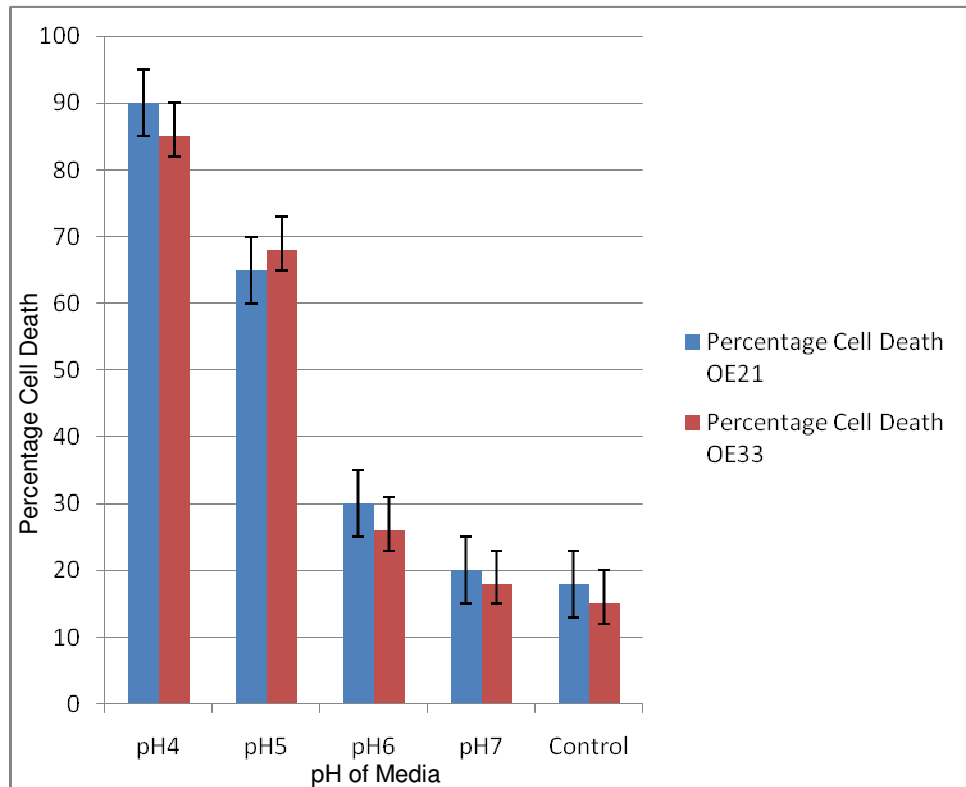


Figure 3.9 Trypan blue stained OE21 and OE33 pH 5-7 treated cells

An estimate of percentage cell death following culture in pH media for OE21 and OE33 cells (calculated by standard deviation from triplicate experiments). These values were based on field of view counts of trypan blue stained cells *in situ*, during cell imaging. Neither cell type grew well or survived below pH 6.

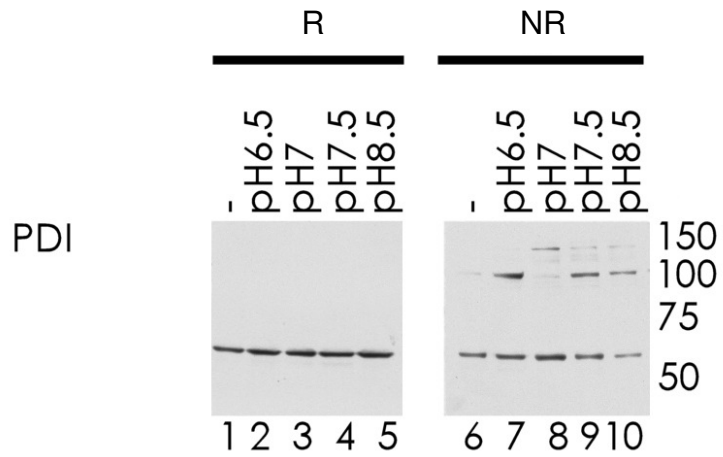


Figure 3.10 PDI expression in HT1080 cells following 24 hour pH 6.5-8.5 treatments

HT1080 cells were treated with altered pH media, and compared with untreated media (shown in lanes 1 and 6) over a 24 hour period. Reducing and non-reducing gels are shown. High molecular weight bands can be seen in the non-reducing gel.

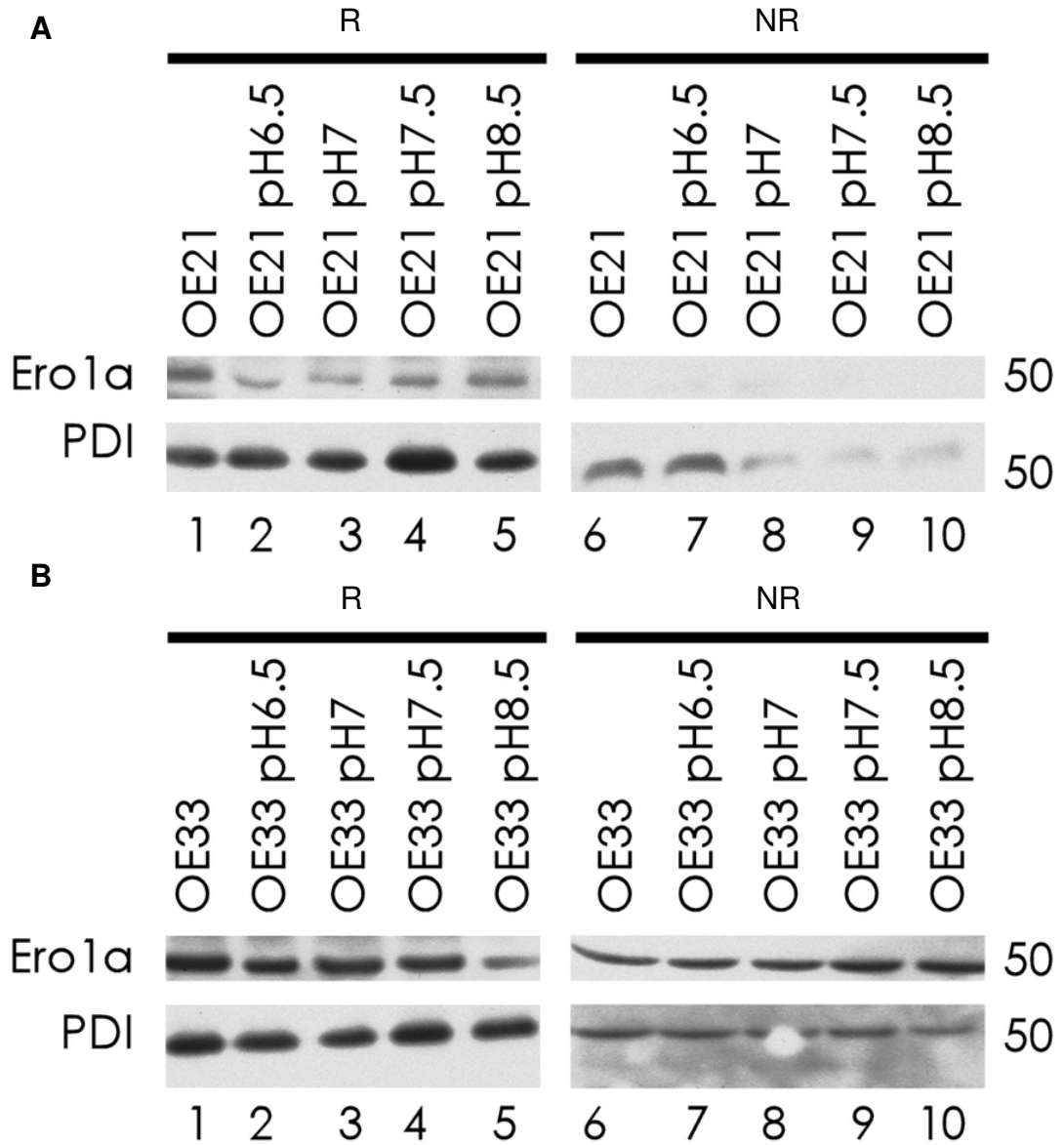


Figure 3.11 PDI and Ero1α expression in OE21 and OE33 following pH 6.5-8.5

treatments

Western blot for Ero1α and PDI in A: OE21 and B: OE33 cell lines, under reducing and non-reducing conditions following pH 6.5-8.5 media treatments. Untreated negative controls are shown in lanes 1 and 6.

### 3.3.2 Simulating reflux with the bile acids deoxycholic acid and chenodeoxycholic acid

The bile salts deoxycholic acid (DCA) and chenodeoxycholic acid (CDC) have been shown to induce cellular proliferation in a model system of Barrett's adenocarcinoma and have been detected in human gastric acid refluxate (Nehra *et al.*, 1999, Stamp, 2002). To assess whether exposure to DCA or CDC causes a change in expression or oxidation state of Ero1 $\alpha$  and the other proteins of interest, HT1080, OE21 and OE33 cells were treated with DCA or CDC within physiological ranges and over a series of time points (Nehra *et al.*, 1999, Hu *et al.*, 2007).

Initially, HT1080 cells were treated with a range of DCA concentrations for 15 minutes (0.025, 0.05, 0.1, 0.25, 0.5 and 0.25 mM). No changes in Ero1 $\alpha$  expression or oxidation state were seen, nor were these concentrations toxic within 15 minutes in preliminary experiments (not shown). OE33 cells were then treated with these same concentrations, over a longer period of 24 hours, to examine possible cytotoxic effects or expression/oxidation state changes. Figure 3.12 shows Western blot data for Ero1 $\alpha$ , PDI and ERp57 for OE33 cells treated with DCA. Expression of Ero1 $\alpha$  was unaffected by DCA treatment in these experiments. There were also no major additional oxidation states seen in the NR gel, suggesting that the ER oxidative folding environment was unchanged as a result of treatment. The first lanes of the non-reduced and reducing gels of Figure 3.12 show data from 1mM DCA treatment, which caused cell death manifested as cells detaching from the dish. This resulted in a reduced signal for Ero1 $\alpha$ , but not for PDI or ERp57. The wobble on the ERp57 is likely due to a gel imperfection and does not indicate a change in oxidation state.

Figure 3.13 shows a Coomassie Blue stained gel of selected replicate DCA treated OE33 cells. For this gel, protein sample concentrations were matched using the Bio-Rad DC protein assay. No gross changes in protein expression could be seen in the

OE33 cells after the acid treatment. Repeated experiments at different DCA concentrations confirmed that there was no change in Ero1 $\alpha$  expression, suggesting that Ero1 $\alpha$  cannot be induced following exposure to DCA only.

Figure 3.14A shows reducing and non-reducing gels for treated OE33 cell lysates, matched for protein concentration. There was no evidence that the expression level or oxidation state of Ero1 $\alpha$  changed as a result of treatment, time or DCA concentration.

In the range of concentrations tested, no changes in oxidation state or expression were seen, so the highest non-toxic treatment concentration (0.25mM) was chosen for timed exposures ranging from 15mins to 24 hours (Figure 3.14B).

Figure 3.14B shows reducing gels for OE21 and OE33 cells treated with 0.25mM DCA for 0-24 hours.

There was no evidence of expression induction within the treatment range, in either OE21 or OE33 cells. Note that Ero1 $\alpha$  was still expressed constitutively higher in OE33 compared to OE21, as first shown in Figure 3.4A.

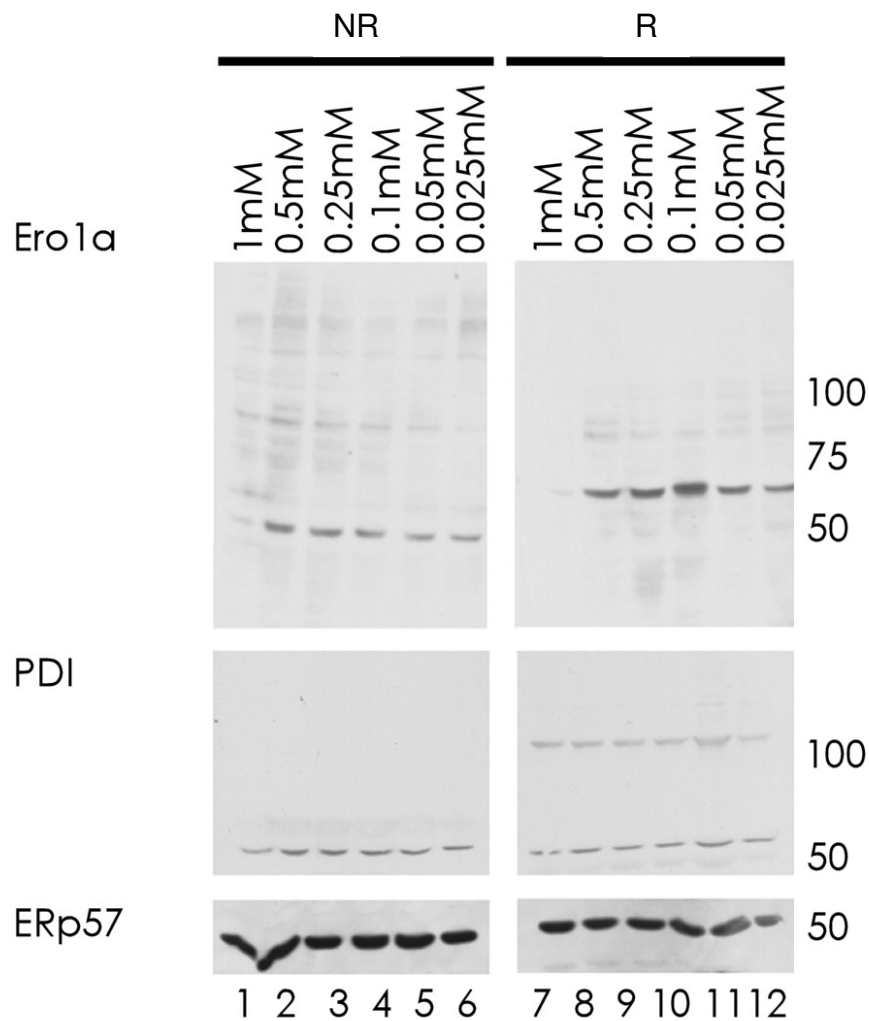


Figure 3.12 OE33 DCA treatments

OE33 cells treated with a range of DCA concentrations, 0.025 mM - 1 mM for 24 hours.

The figure shows Western blot expression data for Ero1 $\alpha$ , PDI and ERp57. There is a slightly lower signal seen in lane 1 for both Ero1 $\alpha$  and PDI blots, due to this treatment being toxic to cells. ERp57 contains no functional disulphide bonds, so expression and oxidation state are the same on both the reducing and non-reducing gel.

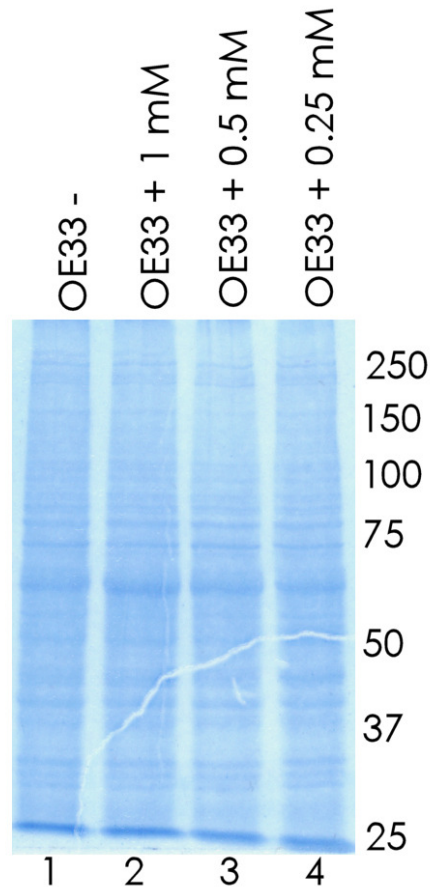


Figure 3.13 OE33 DCA treatments

Coomassie blue stain to show protein sample concentration matching for Western blot.

Although some bile acid treatments caused considerable cell death, lysates were matched for loading, using the Bio-Rad DC protein assay. The lanes showing treated cells (2-4) are matched for protein with the negative control in lane 1.

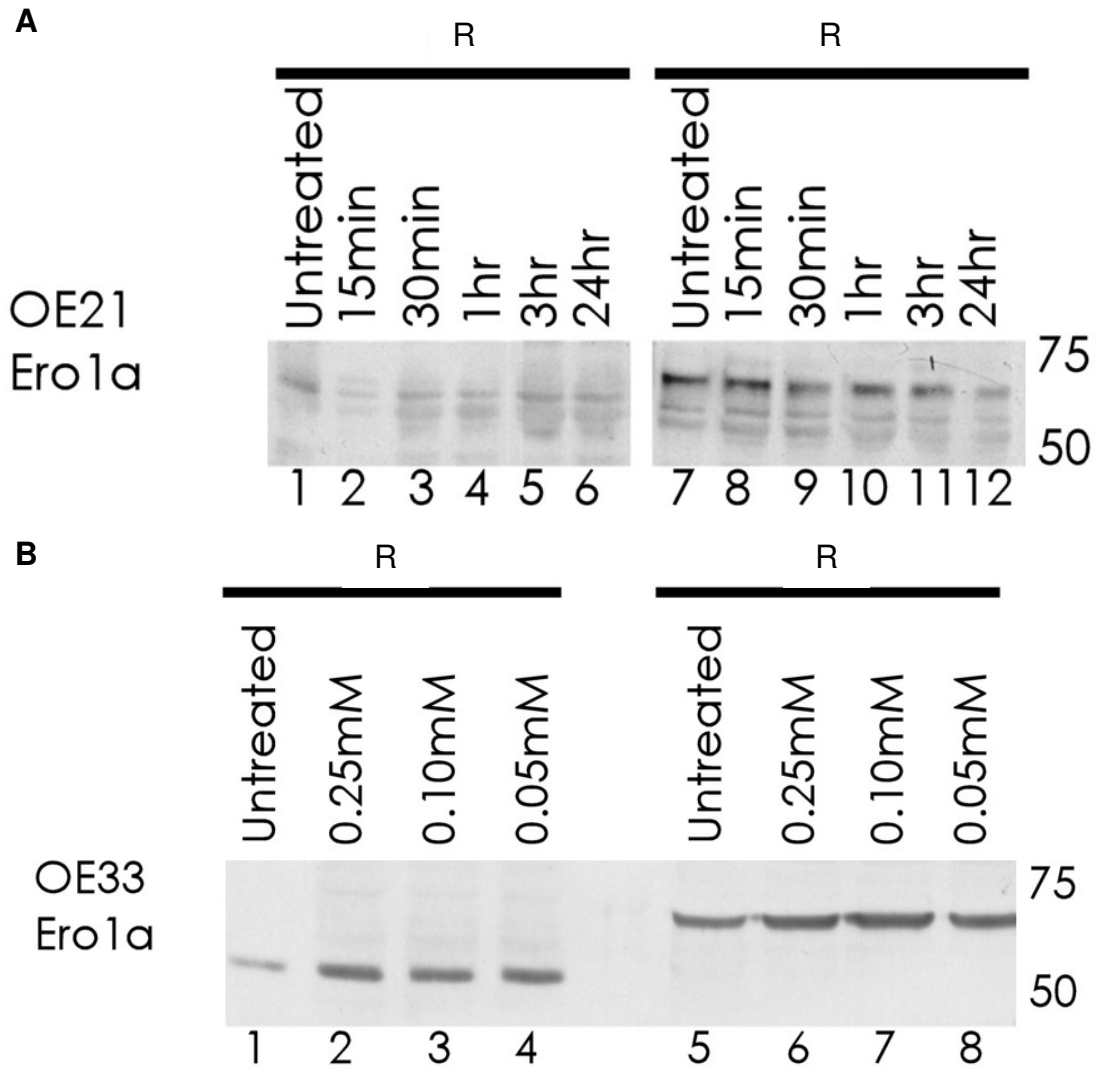


Figure 3.14 DCA time course treatments of OE33 and OE21 cells

A: OE33 cells treated with 0, 0.25, 0.1 and 0.05 mM DCA for 24 hours. B: OE21 (lanes 1-6) cells and OE33 (lanes 7-12) cells treated with 0.25mM DCA in medium for 0-24 hours. Ero1 $\alpha$  is more highly expressed in OE33 cells. Untreated controls are shown in lanes 1 and 5.



Following these experiments with DCA, the bile acid CDC was tested on OE21 and OE33 cells, initially for a 24 hour exposure. Western blot data for Ero1 $\alpha$  and PDI expression are shown in Figure 3.15 and 3.16. As with the DCA treatments, the OE21 cells were more resistant to exposure to 0.5mM CDC compared to OE33. This was reflected in the low signal for Ero1 $\alpha$  in lanes 2 and 8 in both the reducing and non-reducing gels for OE33. The expression of Ero1 $\alpha$  was very low in the OE21 cells and was not induced by treatment (Figure 3.15, note the high non-specific background staining). The PDI blot for OE21 (Figure 3.16, non-reducing gel) shows that a 0.5 mM treatment for 24 hours appeared to increase the signal for a high molecular weight PDI complex at around 100 kDa, whereas for lower concentrations of CDC the 150 kD band was maintained (compare lane 2 with lanes 3-6). These complexes could not be visualised in OE33 cells, but are reminiscent of the complexes seen when HT1080 cells were incubated with different pH media (Figure 3.6). Although the identity of these complexes merits further investigation, it was concluded that bile acid treatment and pH had little effect on the steady state expression levels of the Ero1 $\alpha$  and PDI proteins.

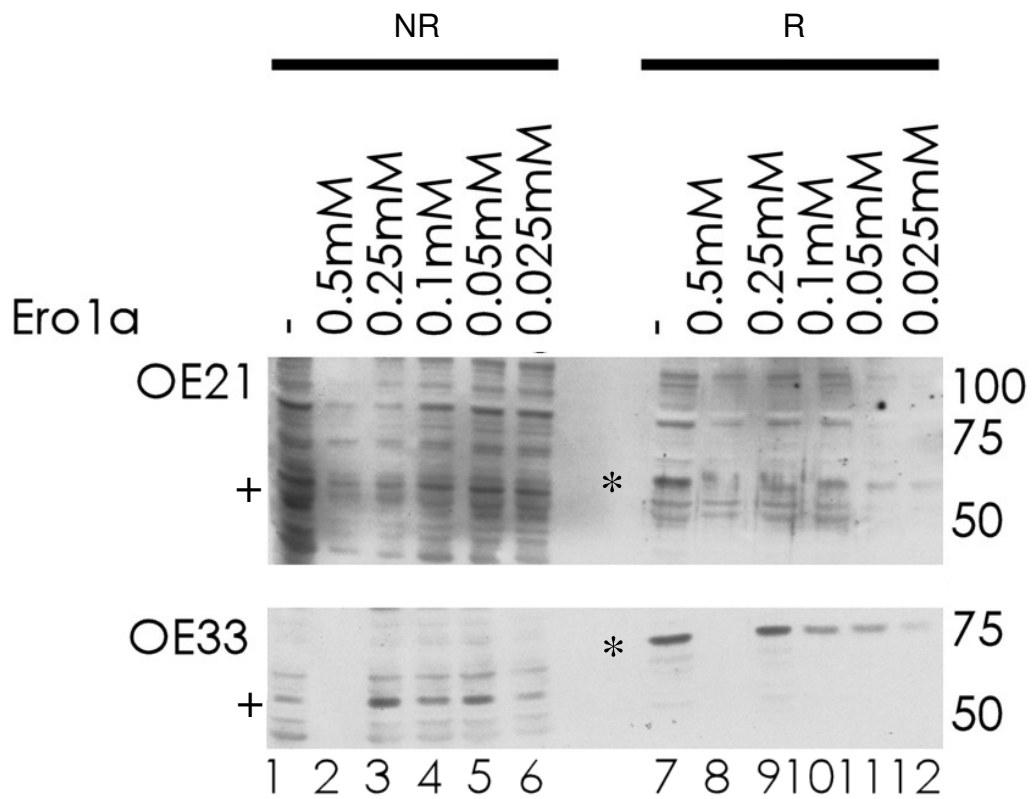


Figure 3.15 Western blot for Ero1 $\alpha$  expression in CDC treated OE cells

A: Western blot data for a CDC titration from 0.5 mM to 0.025 mM, in OE21 and OE33 over a 24 hour time course. Membranes were probed for Ero1 $\alpha$  with D5. High background is sometimes an issue with the D5 antibody used. In the OE33 cells, the 0.5 mM treatment (lanes 2 and 8) caused cell death, and this sample could not be matched to the others. The + shows non-reduced Ero1 $\alpha$ , the \* shows reduced Ero1 $\alpha$ . Untreated negative controls are shown in lanes 1 and 7.

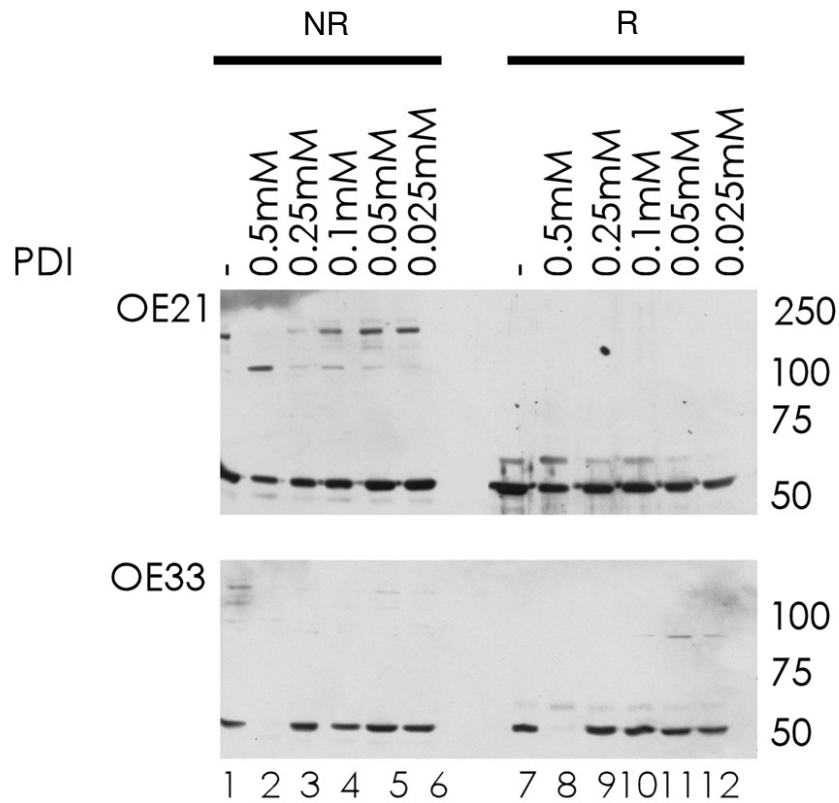


Figure 3.16 PDI expression following CDC titration over 24 hours in OE21 and OE33

Western blot data for PDI following a CDC titration treatment from 0.5 mM to 0.025 mM in OE21 and OE33 over a 24hour time course. The untreated control is shown in lane 1.

### 3.4 Expression of PDI homolog, AGR2

The PDI homolog AGR2 (aka Hag 2; see Ellgaard and Ruddock, 2005) has been shown to be essential for the production of intestinal mucus (Park *et al.*, 2009), and has also been shown to be downregulated in adenocarcinoma (Lee *et al.*, 2005), with the suggestion that functional AGR2 is a key survival factor in Barrett's metaplasia (Pohler *et al.*, 2004).

OE33 cells have been shown to express the mucin MUC4 by immunohistochemistry using cell pellet sections, and by staining with alcian blue, which detects mucins (Mariette *et al.*, 2004). In turn, expression of MUC4 was shown to be upregulated by bile acid treatment including deoxycholic acid, chenodeoxycholic acid, taurocholic acid and taurodeoxycholic acid. The association of MUC4 with AGR2, where AGR2 forms mixed disulphides with disulphide rich mucins, shown by Park *et al.*, 2009, suggested therefore that OE33 cells could also express AGR2, which could be compared with the non-oesophageal adenocarcinoma line, OE21.

To investigate this, cell sections were prepared as outlined in Park, *et al* (see also Chapter 2) and stained for mucins with Alcian blue. This is shown in Figure 3.18A-C. The data reproduced published observations (Mariette *et al.*, 2004), confirming OE33 expression of mucins (dark staining). Such staining was less apparent in the cells derived from oesophageal squamous carcinoma, OE21, and less again in the non-GI cell type, HeLa.

Following this, the expression of AGR2 in each of these three lines was intended to be established by Western blot, with the anti-AGR2 antibody used being that as used for immunofluorescence in Park *et al*. However, at a dilution of 1:500, no signal was seen in any of the three cell types, HeLa, OE21 and OE33 (data not shown).

The three cell lines were probed for AGR2 using immunofluorescence microscopy, to examine AGR2 expression, similar to that in the immunofluorescence work of Mariette *et al.*, 2004 who showed ER localisation of AGR2 in mouse intestinal villi cells. Initially, PDI was used as a positive control for the ER localisation as shown by immunofluorescence. Figure 3.18 confirms such ER localisation of PDI in OE21 (Figure 3.18B), DAPI stained nuclei (Figure 3.18A), a fluorescent signal from PDI, and finally the merge, which shows PDI localised around the cell nuclei in the extensive network of the ER (Figure 3.18C). Figure 3.19 expands on this by confirming PDI expression and ER localisation of PDI in HeLa, OE21 and OE33 (merged images only). Images of OE33 were difficult to obtain because the cells tended to grow in clumps. Having established that PDI could not be seen in immunofluorescence microscopy, AGR2 was examined in the same way. Figure 3.20A-C shows merged images representative of HeLa, OE21 and OE33. Unlike the characteristic ER-localised signals seen from PDI in Figures 3.18 and 3.19, ER staining was not seen with AGR2. Each cell type showed a similar non-specific staining. With the lack of an available positive control for AGR2 in these experiments, it remains possible that AGR2 is expressed at a low level in OE33 cells, or that the antibody does not recognise AGR2 in these cell types. Future experiments with alternative AGR2 antibodies should help address this issue.

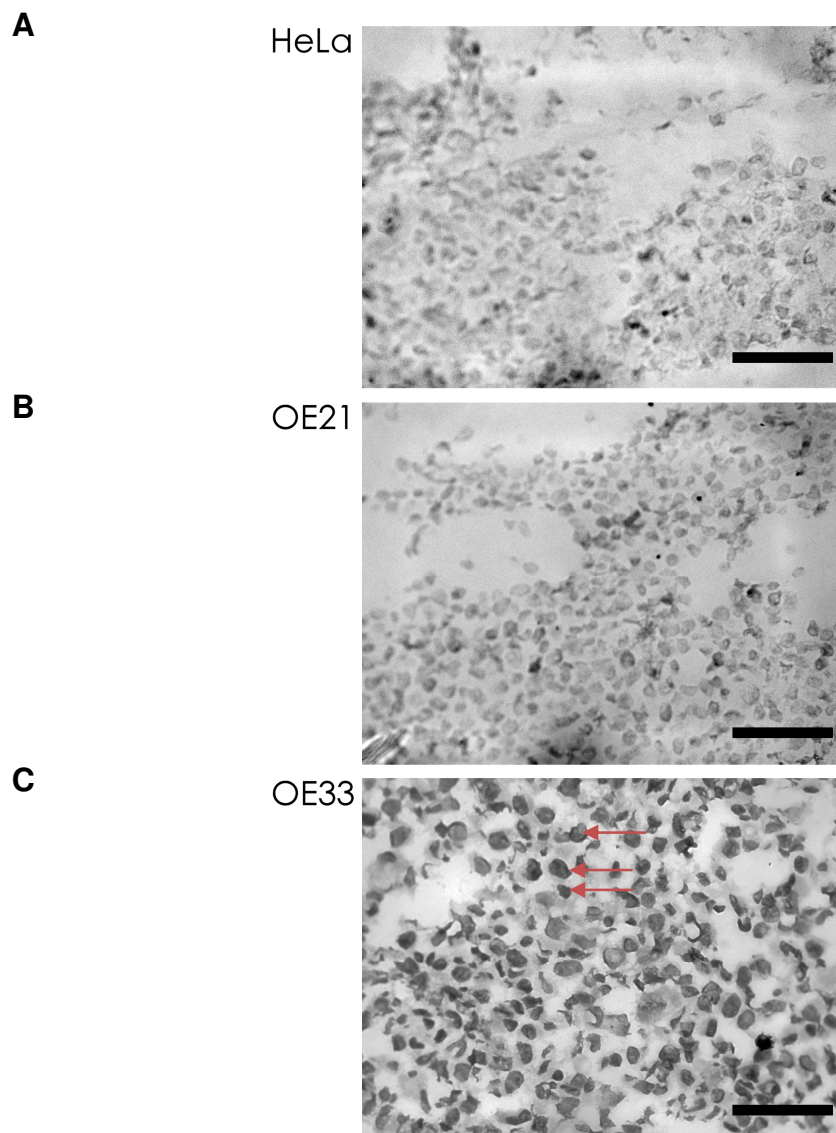


Figure 3.17 Alcian blue staining in HeLa, OE21 and OE33

Alcian blue staining of A; HeLa, B; OE21 and C; OE33. Each sample is derived from a dish of healthy, untreated cells. Mucins stain dark, and some representative cells containing mucins are shown with arrows. Scale bars: 100  $\mu$ m.

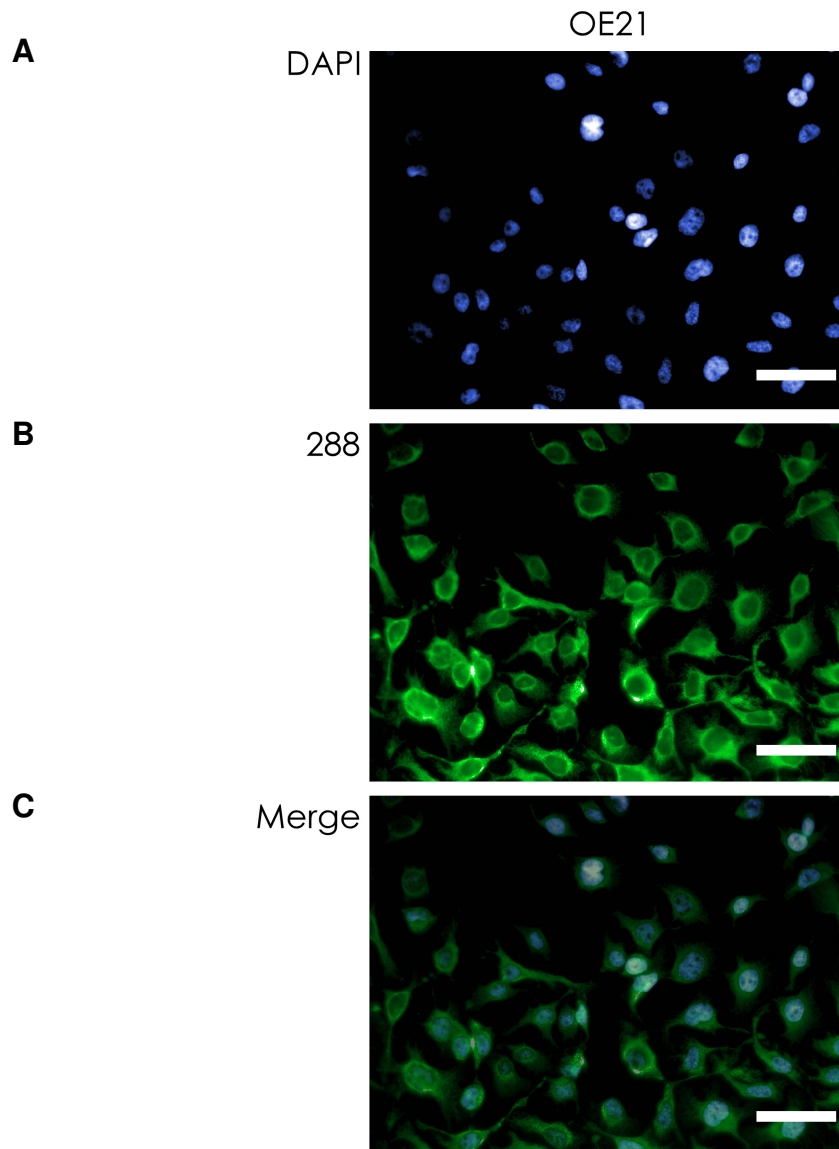


Figure 3.18 Immunofluorescent staining of OE21 for PDI

A: This shows DAPI staining of untreated OE21 cells, showing blue cell nuclei; B: The same cells, showing a strong green fluorescent signal for PDI; C: Merged image of A and B, showing localisation of PDI in the ER around cell nuclei. Scale bars: 50  $\mu$ m.

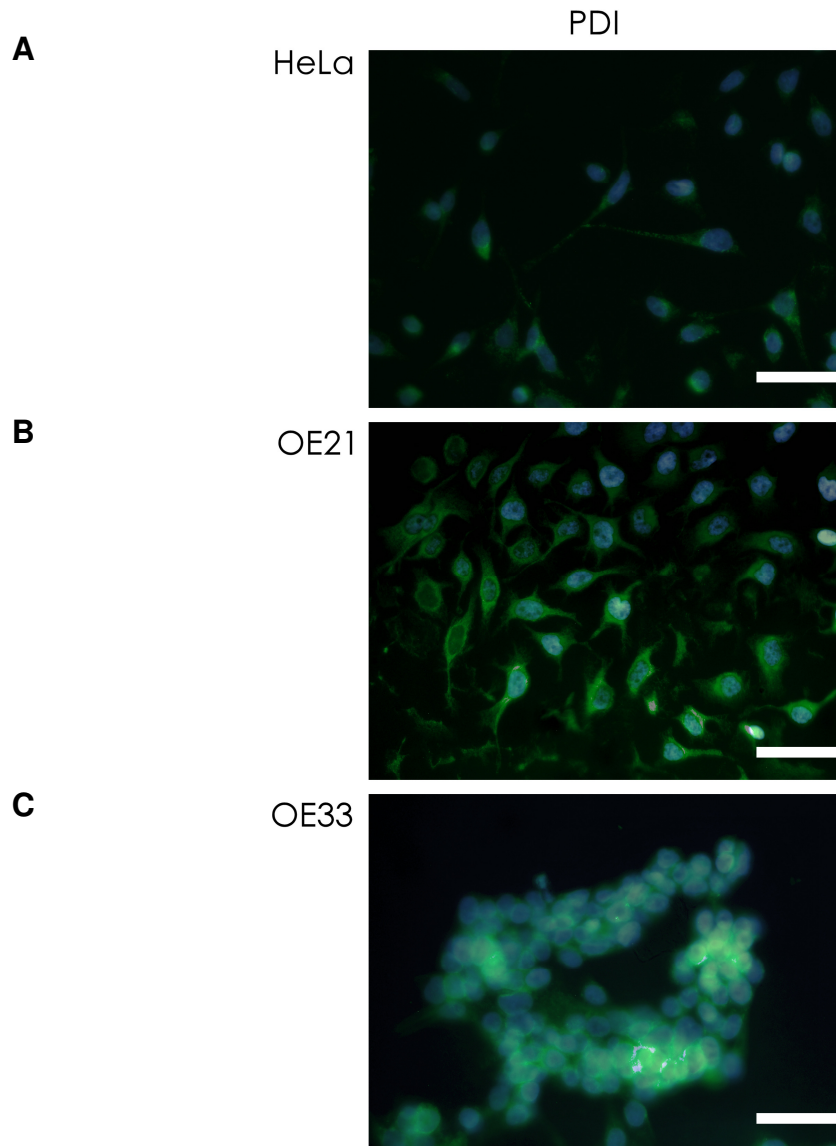


Figure 3.19 Immunofluorescent staining of HeLa, OE21 and OE33 for PDI

A: Merged image showing PDI staining in untreated HeLa cells; B: Merged image showing PDI staining in OE21 cells; C: Merged image showing PDI staining in OE33 cells (note the clumped growth of OE33 leads to a large green PDI glow around in the ER around cell nuclei). Scale bars: 50  $\mu$ m.



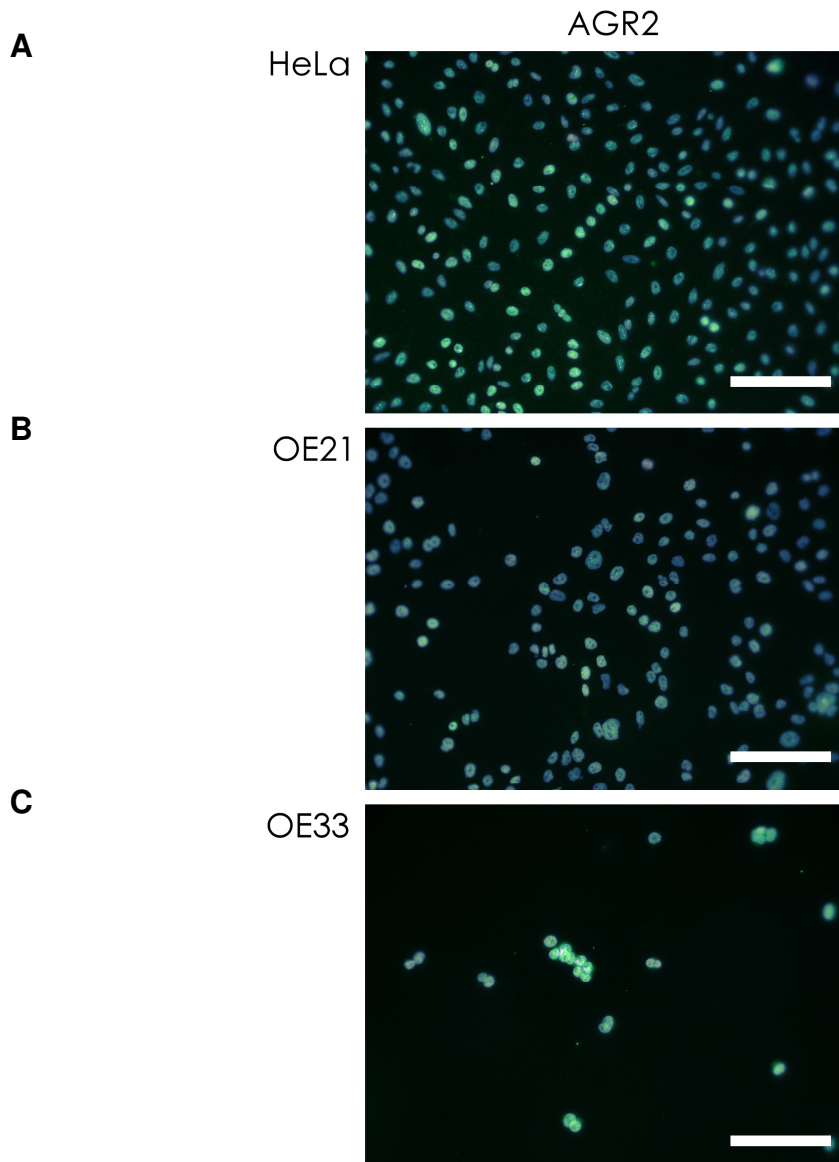


Figure 3.20 Immunofluorescent staining of HeLa, OE21 and OE33 for AGR2

A: Merged image showing absence of AGR2 staining in HeLa cells; B: OE21 cells, and C: OE33 cells. Each sample is from untreated cells. Note that clumped growth of OE33 often lead to a loss of cells. Scale bars: 100  $\mu$ m.

### 3.5 Discussion

In this chapter, Ero1 $\alpha$  has been shown to be expressed constitutively higher in oesophageal adenocarcinoma cells (OE33) compared to oesophageal squamous carcinoma cells, and the non-GI cell lines HeLa and HT1080, by Western blot (Figure 3.4A). This increased expression was not associated with Ero1 $\alpha$  existing in alternate oxidation states, this observation was consistent across multiple experiments, and with different Ero1 $\alpha$  specific antibodies, including monoclonal antibody 2G4 and polyclonal antibody D5. The Ero1 $\alpha$  expressed in OE33 was present in the OX2 compact form, (trapped by alkylation during cell lysis) and has redox active disulphides that can be reduced by DTT *in vitro* (Figure 3.3). Recent functional data suggests that the activation of Ero1 $\alpha$  is directly related to levels of PDI (Appenzeller-Herzog *et al.*, 2010, Inaba *et al.*, 2010); despite the relative differences of Ero1 $\alpha$  expression between OE21 and OE33, no difference in PDI expression was seen between these cell lines (Figure 3.4B).

There was no difference in the expression or oxidation of PDI between OE21 and OE33, or in the expression of PDI family member, ERp57 (Figure 3.4B and C). This was consistent in multiple experiments. However, alcian blue staining of OE33 suggested the presence of disulphide-rich mucins (Figure 3.17). The PDI homologue AGR2 has recently been suggested to be involved in the quality control of mucins in the gut, as evidenced by the AGR2 $^{-/-}$  mice (Park *et al.*, 2009). However, AGR2 in the present work could not be identified by Western blot, or by immunofluorescence in OE33 cells (Figure 3.20). However, PDI expression could be demonstrated both in Western blot and in immunofluorescence, showing that it also localises as expected to the ER in oesophageal cancer cells (Figure 3.18). Despite initial suggestions that OE33

cells could tolerate low pH (Figure 3.6), cell viability assays showed that they could tolerate a margin of between and pH 6 and 7, but not lower (Figure 3.8).

In simulating the gastric reflux environment, either by altering the pH of the cell culture media or by adding bile acids, no change in expression or oxidation state of Ero1 $\alpha$  or PDI can be seen, suggesting that these proteins are not regulated or affected by such agents, either at measured fatal or non-fatal doses (Figures 3.12 to 3.16).

This chapter focused primarily on Ero1 $\alpha$ . To date, the most well-characterised of the human Eros. One of the difficulties in studying Ero1 $\beta$  in cell lines is the lack of a good monoclonal antibody. The Ero1 $\beta$  polyclonal developed by the Benham group (Dias-Gunasekara and Benham, 2005, Dias-Gunasekara *et al.*, 2005) has been useful for determining tissue specific expression in tissue immunohistochemistry. However, both it and the commercial Ero1 $\beta$  antibody (Proteintech "11261-2-AP") were unable to confirm putative Ero1 $\beta$  expression in either OE21 or OE33 (not shown). The potential role of Ero1 $\beta$  is far from well understood in these tissues. The tonic effect of gastric refluxate in the reflux environment, and changes in the cellular oxidative environment described above may explain the preliminary observation that Ero1 $\beta$  is highly expressed in oesophageal tumours (via immunohistochemistry), which is induced by the UPR (Dias-Gunasekara and Benham, 2006-2007).

As such, the purification of recombinant Ero1 $\beta$  was warranted, with the goal of determining further its biochemical properties and using it as the basis for monoclonal antibody production.